Nanoscale

Accepted Manuscript

This article can be cited before page numbers have been issued, to do this please use: K. Joya, Z. Ahmad, Y. F. Joya, A. T. Garcia-Esparza and H. de Groot, *Nanoscale*, 2016, DOI: 10.1039/C6NR03147A.

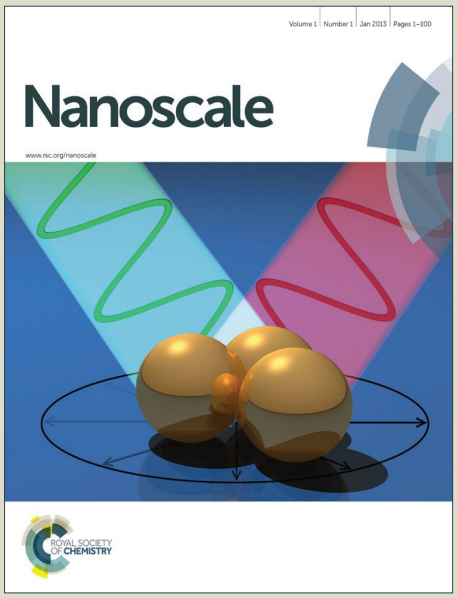

This is an *Accepted Manuscript*, which has been through the Royal Society of Chemistry peer review process and has been accepted for publication.

Accepted Manuscripts are published online shortly after acceptance, before technical editing, formatting and proof reading. Using this free service, authors can make their results available to the community, in citable form, before we publish the edited article. We will replace this *Accepted Manuscript* with the edited and formatted *Advance Article* as soon as it is available.

You can find more information about *Accepted Manuscripts* in the Information for Authors.

Please note that technical editing may introduce minor changes to the text and/or graphics, which may alter content. The journal's standard Terms & Conditions and the Ethical guidelines still apply. In no event shall the Royal Society of Chemistry be held responsible for any errors or omissions in this *Accepted Manuscript* or any consequences arising from the use of any information it contains.

ROYAL SOCIETY OF CHEMISTRY

www.rsc.org/nanoscale

View Article Online
DOI: 10.1039/C6NR03147A

Nanoscale

RSCPublishing

ARTICLE

Efficient electrochemical water oxidation in neutral and near-neutral systems by nanoscale silver-oxide catalyst

Cite this: DOI: 10.1039/xoxxoooooox

Received ooth January 2012,
Accepted ooth January 2012

DOI: 10.1039/xoxxoooooox

www.rsc.org/

Khurram S. Joya*[abc], Zahoor Ahmad[b], Yasir F. Joya[d], Angel T. Garcia-Esparza[c] and Huub J. M. de Groot[a]

In electrocatalytic water splitting systems pursuing for renewable energy using sun light, developing robust, stable and easy accessible materials operating under mild chemical conditions is pivotal. We present here unique nano-particulate type silver-oxide (**AgOx-NP**) based robust and highly stable electrocatalyst for efficient water oxidation. The **AgOx-NP** is generated in situ in a HCO_3^-/CO_2 system under benign conditions. Mircographs show that they exhibit nanoscale box type squared nano-bipyramidal configuration. The oxygen generation is initiated at low overpotential, and a sustained O_2 evolution current density of > 1.1 mA cm^{-2} is achieved during prolonged-period water electrolysis. The **AgOx-NP** electrocatalyst performs exceptionally well in metal-ions free neutral or near-neutral carbonate, phosphate and borate buffers relative to recently reported Co-oxide and Ni-oxide based heterogeneous electrocatalysts, which are unstable in metal-ions free electrolyte and tend to degrade with time and lose catalytic performance during long-term experimental tests.

1. Introduction

World primary energy demand of 14 TW is expected to double by 2050. Carbon based fossils do not seem to be the solution, so there is an enormous effort to come up with energy carriers that are renewable, and can be obtained from low-cost and widespread materials.[1] Water is present worldwide, and it is a cheap and rich source of electrons and protons. By efficiently harnessing sunlight, ubiquitous water molecules can be oxidized to produce electrons and protons, and effectively converted into renewable fuels.[1-2] Thus, the light-driven water transformation into cheap energy carriers is possible through cost effective electrocatalytic and photo-electrochemical (PEC) systems.[3-4] Electrochemical and photoelectrochemical water splitting systems to make hydrogen and oxygen with high efficiency and at a moderate overpotential are vital and energetically very challenging. Besides having an efficient light harvesting and charge separation scheme for a PEC based device, development of robust and active water oxidation catalysts (WOCs) is a principle bottleneck in this pursuit.[5-6] Recently, many molecular complexes of precious metals like Ru and Ir and their oxides along with other inorganic materials of transition metals have been studied for electrocatalytic water oxidation.[7–10] But, due to instability and poor performance, catalytic water oxidation systems are not yet capable of being employed in large scale applications. The overall efficiency of the water oxidation process is largely limited by the slow kinetics of the oxygen evolution reaction (OER) that requires a high overpotential to drive it.[11-12] Thus development of a robust and stable water oxidation electrocatalyst is a key in this regard to make energy conversion device.[11,13]

Thermodynamically, water oxidation requires 1.23 V (vs NHE, pH=0) for its onset, but to drive the process at a faster rate, an extra driving force in the form of overpotential is needed to enhance the reaction kinetics.[5,12] Water electrolysis is conducted at elevated temperature with expensive electrode assemblies in harsh chemical environments, *i.e.* highly acidic or strong alkali media.[6,13] For widespread use, the catalytic materials should be obtained from earth abundant sources and water oxidation needs to proceed under benign conditions.[2,14] A catalytic water oxidation system working at near-neutral pH conditions and at a moderate overpotential would be ideal for application in solar to fuel generation assemblies (Scheme 1).[15] In this quest, non-noble transition metal-oxides derived electrocatalytic systems have attracted scientific interest because of their good catalytic activity for anodic oxygen evolution and abundant availability.[15-17] Catalytic system operating at near-neutral pH condition can be implemented on large terrestrial applications and provides the opportunity to convert water oxidation products (protons and electrons) onto easily storable energy carriers for fuel applications.[15,18] This approach demonstrates an attractive scheme

for direct solar and chemical energy conversion into renewable fuels and clean energy supplies for power generation or automobile application and avoids the problem related to fossils based energy carriers.[19]

In order to establish an electrochemical water splitting system where WOC remains stable in metal free neutral or near-neutral phosphate and borate buffers, or in a CO_2 enriched environment, a water oxidation electrocatalyst is required to operate under pH neutral condition with sustained catalytic activity and high efficiency for oxygen evolution.[15,19] Recently, cobalt and nickel based electrocatalytic materials have been developed *in situ* in neutral or near-neutral carbonate, phosphate and borate buffers, however these electrocatalytic systems are not very stable in metal free phosphate and borate electrolytes, thus limiting their application for long-term catalytic operations for H_2 generation.[17, 20-21] Also, the presence of metal ions in the electrolyte system during water electrolysis may induce its reduction and metal deposition at the reduction site which can block and reduce the active catalyst performance.[15,19] Therefore, there is a need to develop low-cost heterogeneous electrocatalysts which remain stable and effective for long-term catalytic operation in metal-ions free neutral or near-neutral aqueous systems.

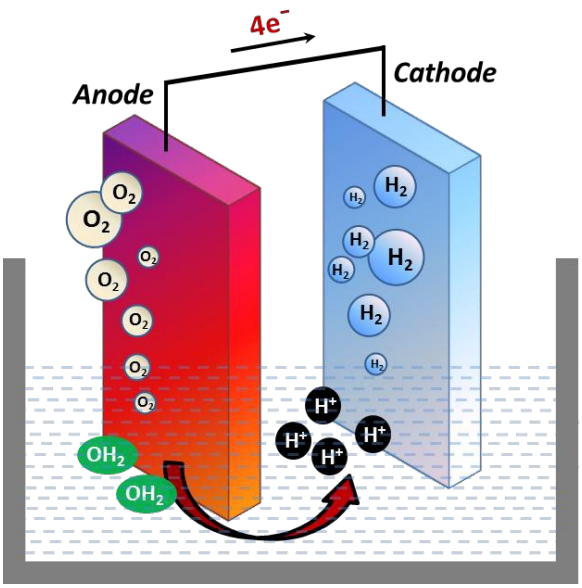

Scheme 1. Schematic representation of water oxidation electrocatalysis (anode) in-combination with a H_2 evolution system (cathode).

Here we report *in situ* generation of a robust and efficient water oxidation electrocatalyst, from easily available silver(I) in neutral bicarbonate electrolyte, that is remarkably stable for prolonged period oxygen evolution process in metal free carbonate, phosphate and borate buffers under pH neutral conditions. The silver-oxide based nano-particulate type electrocatalyst (**AgOx-NP**) was developed on ITO (Indium tin-oxide) or on a glassy carbon disk via anodic electrodeposition from Ag^+ solution in a HCO_3^-/CO_2 system. Silver ions readily get precipitated in an electrolyte solution with pH=7 or above. Bubbling CO_2 in a bicarbonate system reduces the pH just about neutral (pH=6.8 – 6.9) and facilitates the silver complexation and dissolution, and enables the electrodeposition of a **AgOx-Np** based electrocatalyst as a dark grey layer from Ag^+ - HCO_3^-/CO_2 combination on a conducting substrate such as ITO. The surface-deposited electrocatalytic film of **AgOx-Np** displays high catalytic performance in metal-ions free neutral or near-neutral bicarbonate, phosphate and borate based aqueous solutions during long-term water electrolysis compares to Ni and Co-oxide.

2. Experimental

2.1 Materials

Silver nitrate ($AgNO_3$; 99.999%) and sodium bicarbonate ($NaHCO_3$; 99.5-100.5 %) were purchased from Sigma Aldrich. Phosphate and borate buffer solutions are prepared as described previously.[8] carbon dioxide gas (CO_2; 99.999%) was obtained from Linde, B.V. Netherlands. Indium-tin-oxide (ITO) coated glass slides (8-12 Ω/sq surface resistivity) were purchased from Aldrich. A glassy carbon disk (diameter d=0.5 mm) was obtained from Pine research instrumentation. All solutions were prepared in ultra-pure water (Millipore MilliQ® A10 gradient, 18.2 MΩ cm, 2–4 ppb total organic content) and all electrochemical measurements were performed in deoxygenated aqueous solutions at room temperature. The glassware and the electrochemical cells were cleaned and prepared as described previously.[22]

2.2 Electrochemical measurements

For the electrochemical measurements, CO_2 gas was purged (1 atm) through the $NaHCO_3$ electrolyte solution throughout the course of the entire experiment, and at least 25 minutes before each test (pH=6.7–6.8). A three electrode configuration pyrex glass cell was employed for cyclic voltammetry (CV). ITO coated glass slides (1 cm x 2.5 cm, exposed surface area 1.0 cm^2) were used as working electrodes (WE). The ITO electrodes were cleaned and prepared in succession while ultrasonicating with alcohol (isopropanol/MeOH), water and acetone as described previously.[23] The catalytic water electrolysis experiments were carried out in a three electrode double junction H-type glass made electrolysis cell. A platinum wire (thickness: 1 mm), shaped into a spiral, was used as a counter electrode (CE). A silver-silver chloride electrode (SSCE: Ag/AgCl/KCl) was applied as the reference electrode (RE). However, all potentials are referred to a normal hydrogen electrode (NHE). Cyclic voltammetry experiments were performed with an Autolab PG-stat10 potentiostat controlled by GPES-4 software.

2.3 Online oxygen measurements

Oxygen evolution during water oxidation catalysis was monitored by means of online gas chromatography (GC) measurements using micro-GC, T-3000 SRI instruments. A homemade Pyrex glass cell was designed for the online GC analyses with a Teflon based cap having three main slots for three electrodes (WE, CE and RE). There were two more openings in the cap for gas inlet and an outlet for the GC. The gas mixture from the GC-cell was delivered directly to the sampling loop of the gas chromatograph. Sampling points were collected every 10 minutes, and the gaseous products were analyzed using a packed Mol. Sieve 5A coupled with a thermal conductivity detector (TCD). Ar (99.9999%) was used as the carrier gas during the GC measurements.

View Article Online
DOI: 10.1039/C6NR03147A
ARTICLE

2.4 Generation and characterization of nano-particulate type silver-oxide water oxidation electrocatalyst

The **AgOx-NP** electrocatalyst is generated *in situ* from a CO_2 saturated (1 atm) bicarbonate solution (0.1 M – 1.0 M) containing Ag^+ (0.25 mM – 1 mM), on ITO or a glassy carbon disk during constant potential experiment while holding the potential of the working electrode above at 1.3 V (vs. NHE). The catalyst film is also generated during the CV's between 0.0 V – 1.35 V (vs. NHE). A better catalytic coverage is obtained on the anode when deposition was undertaken at a potential avoiding the oxygen evolution on the surface. Interestingly, the **AgOx-NP** catalytic layer does not require the proton abstracting phosphate or borate buffers for electrodeposition and for anodic oxidation of water, as shown to be essential for the generation and electrocatalytic activity of Co-Pi and Ni-Bi based oxygen evolution electrocatalysts.[24] The nano-particulate electrocatalytic silver-oxide was characterized by scanning electron microscopy (SEM), TEM (transmission electron microscopy), X-ray photoelectron spectroscopy (XPS), and energy dispersive X-ray (EDX) compositional measurements and EDX elemental mapping. The so-generated **AgOx-NP** type electrocatalyst is as such for further electrochemical measurements. (The details of the characterization measurements and analyses are described in the supporting information)

3. Results and discussion

3.1 Electro-generation of nano-particulate type silver-oxide water oxidation electrocatalyst

Electrocatalytically active nano-particulate silver-oxide is generated *in situ* on an ITO substrate during controlled-potential electrolysis (CPE) at about 1.40 V vs. NHE, or via cyclic voltammetry (CV) sweeps from 0.1 V to 1.6 V vs NHE in a CO_2 saturated 0.2 M bicarbonate system containing 0.1 – 1.0 mM Ag^+ in a near-neutral pH system (Figure 1a). The anodic CV shows the generation of a large oxidative current wave in the potential region +0.55 V to +0.75 V (vs NHE). This is assigned to the formation of a layer of oxide of silver(I) on the anode surface in the bicarbonate/CO_2 system.[25,26] This catalytic wave declines at 0.71 V (vs NHE) and is followed by a sharp rise at about 1.28 V (vs NHE) ($\eta \approx 450$ mV), along with the generation of tiny oxygen bubbles on the ITO surface. This oxygen generation overpotential is lower than the copper based electrocatalyst generated in bicarbonate electrolytes.[15] On **AgOx-NP** catalytic layer, the oxygen evolution current density attains a value of about 3.5 mA cm^{-2} at 1.60 V (vs NHE), showing a substantial catalytic activity of the **AgOx-NP** type electrocatalyst for the oxygen evolution reaction in a near-neutral HCO_3^-/CO_2 system (Figure 1a). The backward sweep generates a

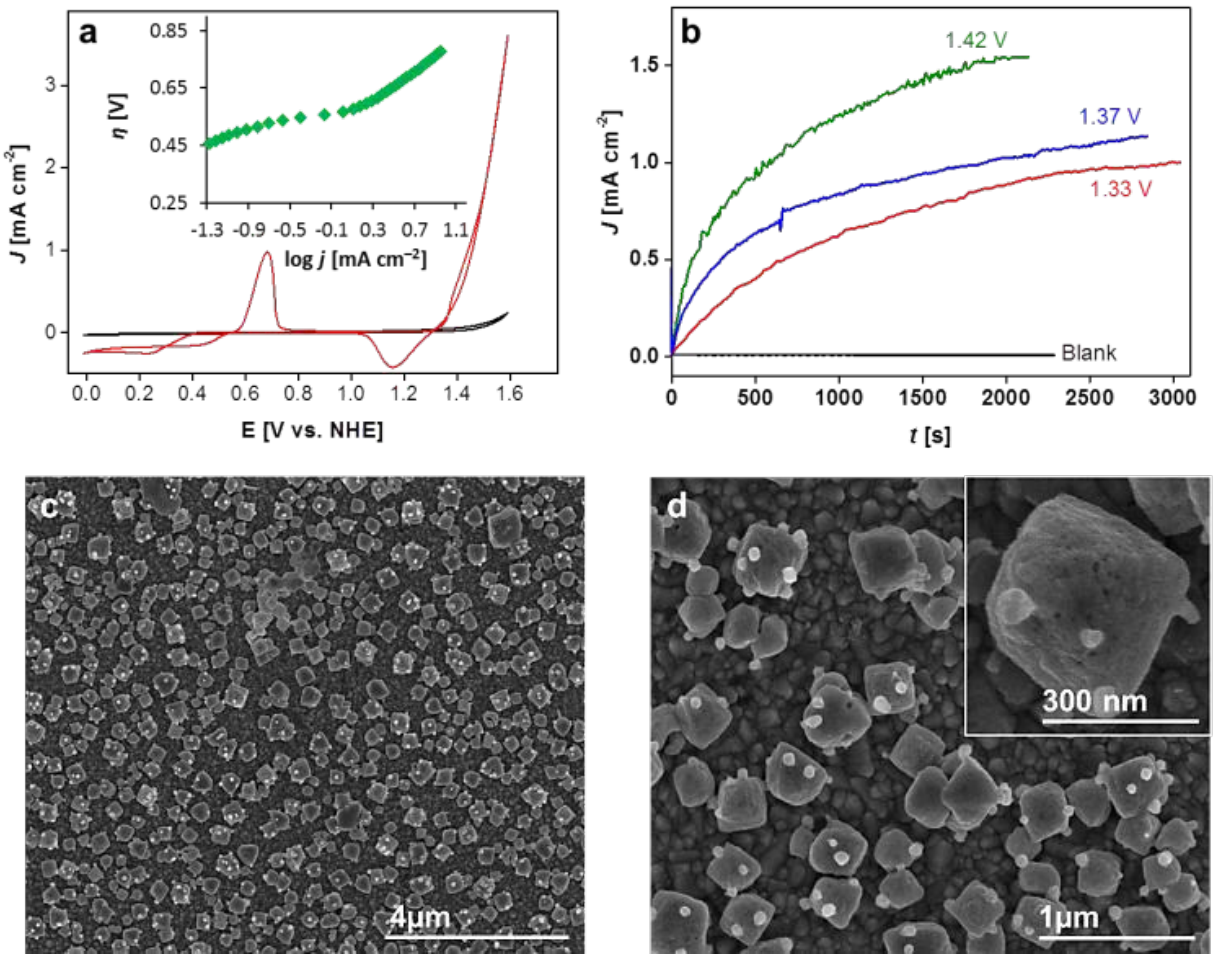

Figure 1. **(a)** Cyclic voltammetry (at scan rate of 50 mV sec^{-1}) and **(b)** Controlled-potential experiment at different potentials for the electro-generation of **AgOx-NP** based electrocatalyst layer on an ITO electrode in a CO_2 saturated 0.2 M bicarbonate electrolyte (pH 6.8–6.9) with 0.5-1.0 mM $AgNO_3$; **(c-d)** Scanning electron microscopy images showing the distribution of electrodeposited **AgOx-NP** on an ITO substrate. Inset Figure 1d shows the enlarged view of a single silver-oxide nanoscale box.

broad reduction wave between 0.99 – 0.81 V vs. NHE (Figure 1a). After successive CVs, a greyish black layer of the silver-oxide catalyst is deposited on the ITO sample. The background current density remains below 45 μA cm^{-2} for the bare ITO substrate. This oxygen evolution onset potential and catalytic current density of the silver-oxide based electrocatalyst are comparable to those observed for Ni-oxide and Co-oxide based materials generated electrochemically in near-neutral conditions.[17,27]

RuO_2 and IrO_2 are the benchmark materials for water oxidation in acidic condition. The catalytic activity data for **AgOx-NP** and RuO_2 and IrO_2 in near-neutral borate buffer show that the **AgOx-NP** sample have comparable oxygen on set and water oxidation activity (Figure S1). However, the **AgOx-NP** electrocatalyst exhibits remarkable long-term stability and activity for water oxidation in metal-free electrolyte compares to Ni-oxide and Co-oxide based materials (we will discuss this comparative analysis in more details in the later section). The current – overpotential (log i vs η) measurements for **AgOx-NP** electrocatalyst in oxygen evolution regime reveal a Tafel slope of 55 mV dec^{-1} represented in the inset Figure 1a. This Tafel slope is lower than observed for NiOx and CoOx based electrocatalysts,[17,20] and represents a mechanism of one proton-one electron transfer simultaneously leading to the onset of oxygen evolution during water oxidation.[17] A lower Tafel slope also indicates that a smaller potential window is needed to get a current decade which is highly desirable for solar-driven water oxidation.

For the electrodeposition of electrocatalytic **AgOx-NP** during constant-potential electrolysis experiments (at 1.33 V, 1.37 V and 1.42 V vs NHE), the current densities in all cases increase with time indicating gradual formation and growth of the **AgOx-NP** layer on conducting ITO substrate (Figure 1b). At low CPE potential (~1.33 V vs NHE), the initial current density for the generation of catalytic film is low compares to higher potentials deposition run. At higher deposition potential (>1.35 V), the current saturation during deposition also reached at faster rate. Deposition current density above 1.55 mA cm^{-2} at about 1.42 V (vs NHE) indicate the generation of more catalytic site at the anode along with high rate of oxygen generation. After few minutes, a dark catalytic layer is formed on the ITO along with the observation of a rich stream of oxygen bubbles that was coming out of the electrode surface. There is a steady growth in the current reaching > 1.1 mA cm^{-2} in about half an hour of the experiment. This current rise is ascribed to the growth and generation of nanoscale catalytic sites on the catalyst surface that increases the amount of surface active species of the electrocatalytic assembly for water splitting. The small spikes in the CPE current are due to the generation of oxygen bubbles at the silver-oxide catalytic surface (Figure 1b).

3.2 Characterization of electrodeposited nano-particulate type silver-oxide film

The morphology of the electrodeposited grayish black Ag-oxide based catalyst film is examined by scanning electron microscopy as presented in Figures 1c and 1d. For SEM imaging, the catalytic film is developed on the anode by bulk electrolysis at a constant potential of 1.39 V (vs NHE) for 19 minutes in a near-neutral HCO_3^-/CO_2 system containing 0.5 mM $AgNO_3$. Silver-oxide derived electrocatalyst on ITO electrode shows nanostructured particles with fairly homogeneous shape and size that are uniformly distributed on the anode surface (Figure 1c). A magnified SEM view shows squared nano-bipyramidal shaped silver oxide units dispersed on the surface of the anode (Figure 1d). This octahedral elements seem to be constructed starting from smaller nanoparticles in the order of 60–70 nm. The secondary particle size of the AgOx nano-bipyramid is in the range of 300–400 nm and the **AgOx-NP** can be seen individually on the ITO exterior, however there are few particles with a bigger size (up to 500 nm) as well (Figure S2).

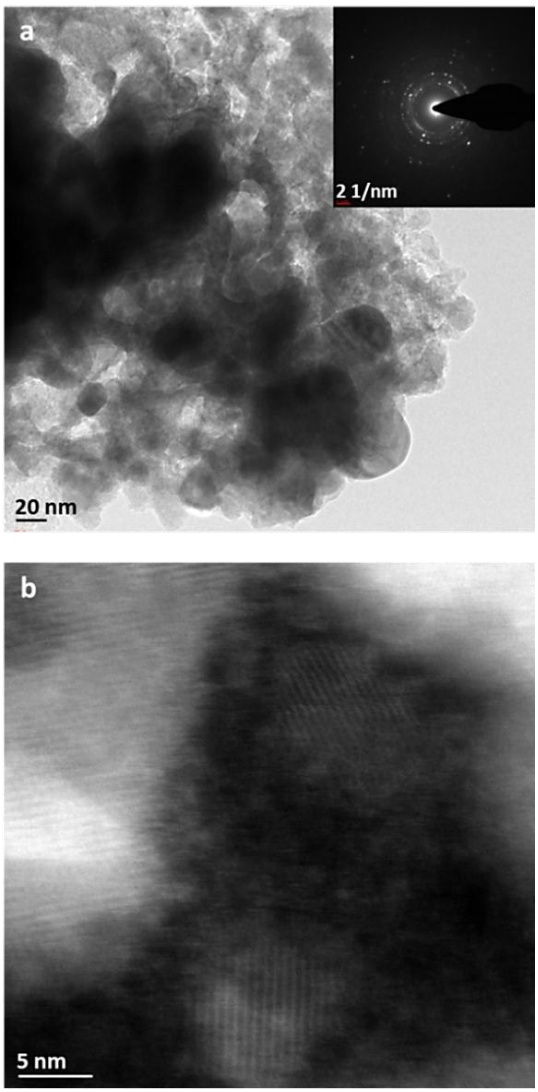

Figure 2. (a) TEM (transmission electron microscopy) image and (b) high resolution TEM for the electrodeposited **AgOx-NP**. (The **AgOx-NP**@ITO based catalyst system is developed by CPE at 1.40 V in a near-neutral HCO_3^-/CO_2 system with 0.5 mM Ag^+).

TEM in bright-field (BF) mode revealed nanoparticulate morphology of Ag-oxide electrocatalytic samples (Figure 2a). The phase of the NPs was confirmed by investigating the diffraction rings present in the selected-area electron diffraction (SAED) which was acquired from the same area and is shown as an insert in Figure 2a. The size of silver oxide nanoparticles and their crystal structure were determined with high-angle annular dark-field (HAADF)

View Article Online
DOI: 10.1039/C6NR03147A
ARTICLE

scanning TEM (STEM) technique and a typical micrograph acquired with this technique is given in Figure 2b. HAADF-STEM analysis showed that the crystal size of those silver-oxide NPs was 7- 8 nm, however irregular distribution of crystal size also observed. Furthermore those NPs were crystalline whose structure matches with the one revealed by SAED analysis.

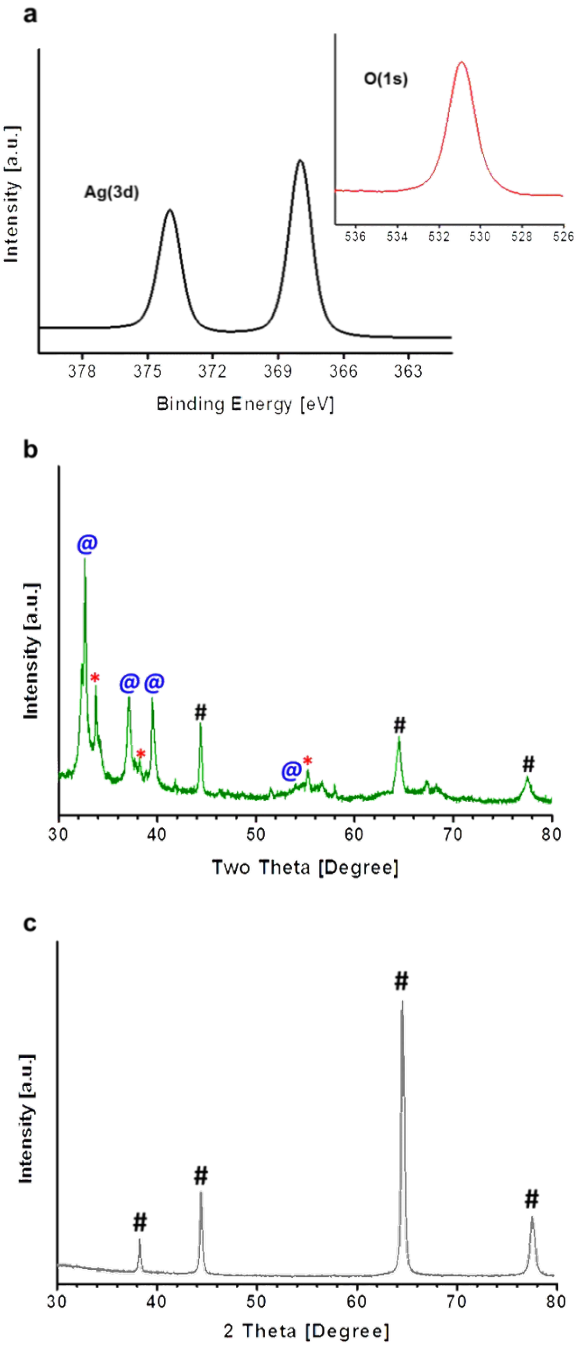

Figure 3. (a) Enlarged view of the XPS (X-ray photoelectron spectroscopy) spectrum for Ag 3d in the electrodeposited catalytic layer of the **AgOx-NP** film on an ITO anode; (b-c) X-ray diffraction (XRD) pattern for the electrodeposited **AgOx-NP** film and for simple Ag substrate. In the XRD spectra, the symbols #, asterisk and @ represent Ag, Ag_2O and AgO (Ag_2O/Ag_2O_3), respectively. (For XPS and XRD analyses, the **AgOx-Np**@ITO based catalyst system is developed by CPE at 1.40 V in HCO_3^-/CO_2 system with 0.5 mM Ag^+).

The surface composition of the **AgOx-NP** was analyzed by X-ray photoelectron spectroscopy. The elemental detection on the XPS survey for the **AgOx** electrocatalyst indicates the presence of silver and oxygen (Figure S3). XPS data show the Ag 3d5/2 peak at 367.9 eV and the Ag 3d3/2 peak at 373.8 eV that are in the characteristic range for silver bound to O and indicative of the AgO type species (Figure 3a).[28] There is a single oxygen binding energy peak centered at 531 eV, indicating the presence of metal bound oxide on the surface. As the catalytic film of **AgOx-NP** is developed in the aqueous phase from Ag^+, there is a possibility for the presence of metal bound -OH type oxide species (528-532).[29] The X-ray diffraction (XRD) pattern for the Ag metal and Ag-oxide sample are shows in Figures 3b-3c. The silver-oxide sample reveals the presence of both Ag_2O and AgO phases in the catalytic layer, with Ag(II) oxide as dominating phase (Figure 3b). It is known that the higher oxide phase AgO usually exists as Ag_2O/Ag_2O_3.[30] There are also some signals representing the contribution from metallic silver phase (Figures 3c), that might have formed via reduction of Ag-oxide in air.

Further, the catalytic nanoscale silver-oxide material is characterized by the Raman spectroscopy (Figure S4). The Raman peaks at 231 cm^{-1}, 300 cm^{-1}, 430 cm^{-1}, 467 cm^{-1}, 708 cm^{-1} and 1059 cm^{-1} represent the presence of AgO phase in the catalytic film. However, the Raman features at 430 cm^{-1}, 467 cm^{-1} and 708 cm^{-1} also indicate that some Ag_2O type materials in the catalytic layer. Thus, this film is a mixture of AgO and Ag_2O with Ag(II) dominance. Further, the bulk elemental composition of the freshly electrodeposited **AgOx-NP** layer was analyzed by energy dispersive X-ray spectroscopy. EDX measurements show the presence of silver, carbon, oxygen as main constituent elements in the **AgOx-NP** film (Figure S5). Compositional analyses of the **AgOx-NP** EDX reveal a Ag:C ratio of 6:1. Hence the electrodeposited **AgOx-NP** contains about 11 percent of carbon contents in the catalyst layer. Carbon assimilation in metal-oxide matrix is thought to induce high surface area in the catalytic deposit while facilitating good electron transport and enhanced structural flexibility.[17a,31] EDX elemental mapping clearly show the distribution of silver, oxygen and carbon in the catalytic layer (Figure S5). The distribution of silver and oxygen in the catalytic matrix is very homogeneous, and there is more carbon contribution (from the carbonate system) on the surface then the bulk indicating the physical adsorption of the carbonate ions on the metal oxide surface during the deposition and/or catalytic operation. There are few nanoscale holes in the catalytic deposit, and carbon contents are more pronounced around that region in the EDX mapping image (Figure S6).

3.3 Water oxidation performance of the nanoscale silver-oxide electrocatalyst

The long-term stability and catalytic performance of the **AgOx-NP** type electrocatalytic material, prepared on ITO by constant-potential electrolysis from Ag^+ in neutral bicarbonate solution, was tested in a clean electrolyte system (Figure 4). The electrocatalytic **AgOx-NP**@ITO system is also active for OER in the presence of silver ions in HCO_3^-/CO_2 solution, with an oxygen evolution current density approaching > 1.1 mA cm^{-2} in one hour and sustained for many hours of CPE (Figure S7). The **AgOx-NP**@ITO catalytic system is then subjected to a silver free HCO_3^-/CO_2 solution, and the water oxidation experiment is conducted at 1.39 V (vs. NHE;

pH=6.9). Interestingly, a very stable current density of > 1.2 mA cm^{-2} is achieved that is stable for many hours without noticeable decrease in the performance (Figure 4a). There was a rich steam of oxygen bubbles coming out from the anode surface. Surprisingly, the anodic performance of **AgOx-NP** in neutral pH does not require the proton abstracting phosphate or borate buffers for water oxidation, as was shown to be essential for the formation and activity of cobalt-phosphate (Co-Pi) and nickel-borate (Ni-Bi) based electrocatalysts.[17]

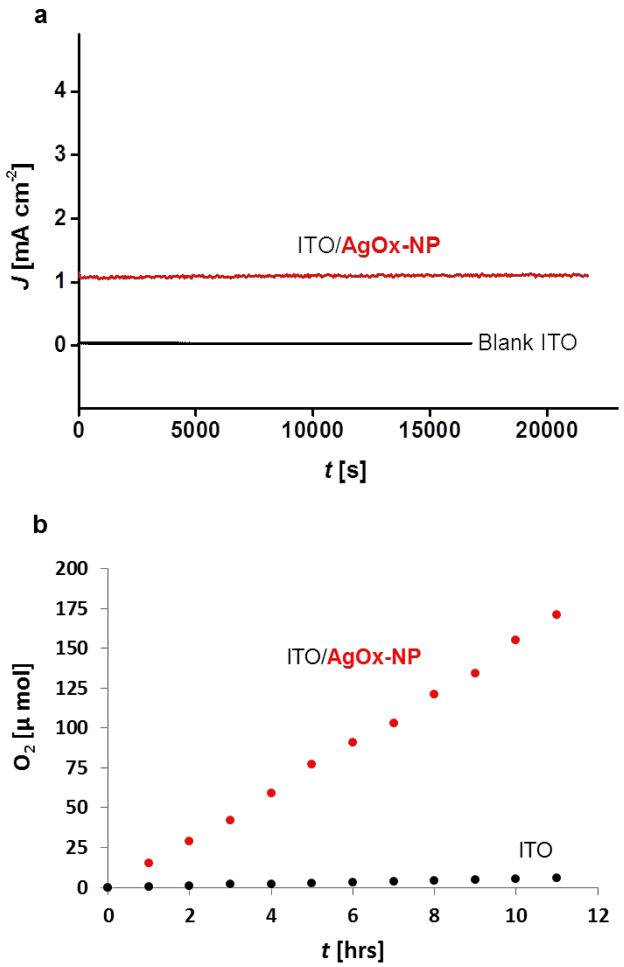

Figure 4. (a) Controlled-potential water electrolysis with a clean blank ITO and with a **AgOx-NP**@ITO based electrocatalyst system in deoxygenated and CO_2 saturated 0.2 M bicarbonate solution without additional Ag^+ (pH=6.8-6.9) at a constant-potential of 1.39 V (vs. NHE). (**b**) Online oxygen measurements during long-term controlled-potential water electrolysis in CO_2 saturated bicarbonate electrolyte. (The **AgOx-NP**@ITO based catalyst system is developed by CPE at 1.40 V in a near-neutral HCO_3^- /CO_2 system with 0.5 mM Ag^+).

Following long-term electrolysis tests, online oxygen generation measurements for **AgOx-NP**@ITO catalytic system are also conducted in HCO_3^-/CO_2 based electrolyte. Online gas chromatographic (GC) measurements using a micro-GC (Figure S8) show that electrocatalytic water oxidation test for 11 hours of electrolysis has yielded more than 170 µmol of molecular oxygen in 11 hours of CPE operation (Figure 4b). This can be translated into an oxygen generation rate of 15.5 µmol of oxygen gas per hour coming out of 1 cm^2 area of the **AgOx-NP**@ITO catalytic surface. Counting the total charge passed through the system during electrolysis, a Faradaic efficiency of > 98 % is observed by taking into account that the current is generated due to $4e^-$ water oxidation involving two OH_2 molecules to make one O_2 molecule. Apparently, there was no oxygen detected during the water electrolysis using only bare ITO substrate (Figure 4b). The remarkable activity of the **AgOx-NP** catalytic system for long-term water oxidation is very promising and provides a new opportunity in developing neutral pH based electrocatalytic assemblies for anodic oxygen generation.

3.4 Long-term water electrolysis in phosphate and borate aqueous buffers

The Recently, proton abstracting phosphate and borate aqueous buffers are reported as active systems for cobalt and nickel based electrocatalysts.[17] However, it is important to note that Co-Pi and Ni-Bi lost their anodic activities in metal free clean phosphate and borate electrolytes.[20-21] So, the continuous presence of Co or Ni ions in phosphate or borate aqueous buffers is necessary for the sustained activities of these catalysts. These results lead us to test the performance of **AgOx-NP** for anodic water oxidation in metal ions free phosphate (pH=7.1) and borate (pH=9.2) solutions.

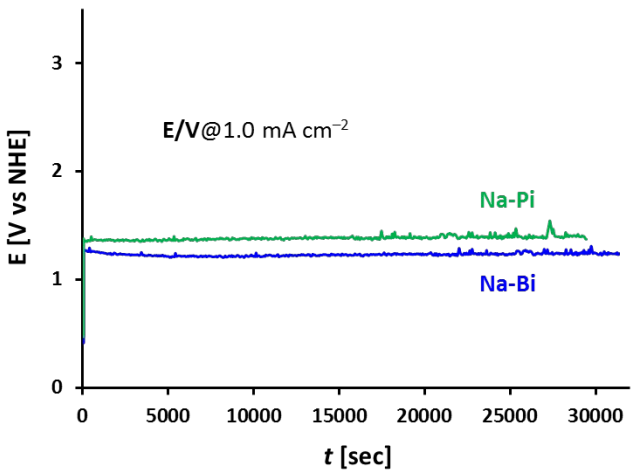

Figure 5. Long-term constant-current electrolysis (chronopotentiometry) for **AgOx-NP@ITO** in deoxygenated 0.2 M phosphate (pH=7.1) and borate (pH=9.2) buffer solutions at controlled current of 1.0 mA cm^{-2}. (The **AgOx-NP**@ITO based catalyst system is developed by CPE at 1.40 V in a near-neutral HCO_3^-/CO_2 system with 0.5 mM Ag^+).

We employed the constant-current water electrolysis (chronopotentiometry) experiments to investigate the performance at a constant current density of 1.0 mA cm^{-2}, and monitored the voltage response of the system to maintain that current density. Interestingly, in oxygen free aqueous sodium-phosphate (Na-Pi) and sodium-borate (Na-Bi) electrolytes, the **AgOx-NP** electrocatalyst remains amazingly stable for water oxidation. At 1.0 mA cm^{-2} current in neutral Na-Pi buffer, a constant steady-state potential of ~ 1.37 V (vs. NHE) is preserved for more than 10 hours of the catalytic test (Figure 5). In pH=9.2 Na-Bi buffer, a steady ~ 1.25 V (vs. NHE)

View Article Online
DOI: 10.1039/C6NR03147A
ARTICLE

potential is observed to abstract a 1.0 mA cm^{-2} current density for water oxidation. In both metal free phosphate and borate systems, there is no significant change in the voltage, which is a direct indication of the stability and good catalytic activity of the **AgOx-NP** electrocatalyst for anodic water oxidation. A comparative analysis of the electrochemical water oxidation OER activities and Tafel slopes of electrodeposited RuO_2, IrO_2, CoOx and NiOx based materials are given in Table S1. The catalytic performance testing during anodic water oxidation shows that the activity of **AgOx-NP** electrocatalyst is comparable to that of benchmark RuO_2, IrO_2. However, the electrodeposited CoOx and NiOx based materials have much lower activities compare to **AgOx-NP** electrocatalyst sample. Also CoOx and NiOx exhibit much higher Tafel slopes relative to **AgOx-NP** based anodic catalyst. A standard current density of 10mA cm^{-2} is obtained under 600 mV whereas CoOx and NiOx show much higher overpotentials to achieve those high current densities.

4. Conclusions

To make renewable hydrogen and other nonfossil carbon base alternative energy carrier via water splitting route, Water oxidation electrocatalyst is desired to operate with high efficiency and at a moderate overpotential. We presented here a unique nano-particulate type silver-oxide based robust electrocatalyst for high activity water oxidation. The electrocatalytic **AgOx-NPs** are developed *in situ* on simple ITO substrates via anodic electrodeposition from a HCO_3^-/CO_2 system containing silver (I) ions. Transition metals based electrocatalytic materials have shown catalytic activities for water oxidation, however their anodic performance are gradually lost in metal free buffers (phosphate and borate) and common electrolytes.[17, 20-21] The nanoscale **AgOx-NP** presented here displays very high catalytic stabilities in metal-ions free neutral or near-neutral bicarbonate, phosphate and borate buffer solutions as compared to recently reported CoOx and NiOx based heterogeneous electrocatalysts. Silver ions quickly precipitate in neutral pH solution. Our unique approach of bubbling CO_2 in a bicarbonate system reduces the pH just below neutral (pH=6.8 – 6.9) and facilitates the silver complexation and dissolution, and enables the electrodeposition of **AgOx-NP** based electrocatalyst on ITO exterior. On **AgOx-NP**@ITO catalytic system, an oxygen evolution current density of > 3.0 mA cm^{-2} is obtained at 1.6 V (vs. NHE; pH=6.8–6.9). During long-term water electrolysis, a stable oxygen evolution current density of > 1.1 mA cm^{-2} is achieved that is sustained for many hours with no noticeable decrease in the performance. During six hours of electrolysis using **AgOx-NP**@ITO catalytic system, 57 µmol of molecular oxygen was generated indicating an attractive Faradaic efficiency of ~ 98 %. This study presents our continuous research in developing efficient and stable water oxidation electrocatalysts that are active, robust and easily accessible in near-neutral conditions, aiming to produce renewable fuels and easily storable energy carriers.[32,35]

Acknowledgements

K.S. Joya acknowledges research funding from the Higher Education Commission (HEC), Government of Pakistan and Leiden University/BioSolar Cells for the research support and facilities. The authors are thankful to Mr. Verhoeven Tiny (TU-Eindhoven) for the XPS experiments and greatly acknowledge the assistance of Dr. Dalaver Anjum (Imaging and Characterization Lab, KAUST) in TEM and related analyses.

Notes and references

[a] Leiden Institute of Chemistry, Leiden University
Einsteinweg 55, P.O. Box 9502, 2300 RA Leiden, The Netherlands.
E-mail: khurram.joya@gmail.com
Fax: (+31) 71-527-4603
[b] Department of Chemistry, University of Engineering and Technology, GT Road 54890 Lahore, Punjab, Pakistan
E-mail: khurram_joya@uet.edu.pk
[c] Division of Physical Sciences and Engineering, KAUST Catalysis Center (KCC), King Abdullah University of Science and Technology (KAUST), 4700 KAUST, Thuwal 23955-6900, Saudi Arabia
[d] Faculty of Materials Science and Engineering, Ghulam Ishaq Khan (GIK) Institute of Engineering Sciences and Technology
Topi 23640, Khyber Pakhtunkhaw, Pakistan

Electronic Supplementary Information (ESI) available: [details of any supplementary information available should be included here]. See DOI: 10.1039/c000000x/

1 K. S. Joya, Y. F. Joya, K. Ocakoglu and R. van de Krol, *Angew. Chem.*, 2013, **125**, 10618; *Angew. Chem. Int. Ed.*, 2013, **52**, 10426.
2 a) N. Morlanés, K. S. Joya, K. Takanabe and V. Rodionov, *Eur. J. Inorg. Chem.*, 2015, **2015**, 49; b) D. G. Nocera, *Acc. Chem. Res.*, 2012, **45**, 767.
3 K. S. Joya and H. J. M. de Groot, *ChemSusChem*, 2014, **7**, 73.
4 K. S. Joya, N. Morlanés, E. Maloney, V. Rodionov and K. Takanabe, *Chem. Commun.*, 2015, **51**, 13481.
5 H. Dau, C. Limberg, T, Reier, M. Risch, S. Roggan and P. Strasser, *ChemCatChem*, 2010, **2**, 724; b) K. Ocakoglu, K. S. Joya, E. Harputlu, A. Tarnowska and D. T. Gryko, *Nanoscale*, 2014, **6**, 9625.
6 M. de Respinis, K. S. Joya, H. J. M. De Groot, F. D'Souza, W. A. Smith, R. van de Krol and B. Dam, *J. Phys. Chem. C*, 2015, **119**, 7275.
7 X. Sala, I. Romero, M. Rodŕguez, L. Escriche and A. Llobet, *Angew. Chem. Int. Ed.*, 2009, **48**, 2842.
8 K. S. Joya, N. K. Subbaiyan, F. D'Souza and H. J. M. de Groot, *Angew. Chem. Int. Ed.*, 2012, **51**, 9601; *Angew. Chem.*, 2012, **124**, 9739.
9 T. Nakagawa, N. S. Bjorge and R. W. Murray, *J. Am. Chem. Soc.*, 2009, **131**, 15578.
10 J. Gao, et al., *Scientific Reports*, 2013, **3**, 1853.
11 P. Du and R. Eisenberg, *Energy Environ. Sci.*, 2012, **5**, 6012.
12 K. S. Joya, L. Sinatra, L. G. AbdulHalim, C. P. Joshi, M. N. Hedhili, O. M. Bakr and I. Hussain, *Nanoscale*, 2016, **8**, 9695.
13 M. G. Walter, E. L. Warren, J. R. McKone, S. W. Boettcher, Q. Mi, E. A. Santori and N. S. Lewis, *Chem. Rev.*, 2010, **110**, 6446.
14 M. Risch, K. Klingan, F. Ringleb, P. Chernev, I. Zaharieva, A. Fischer and H. Dau, *ChemSusChem*, 2012, **5**, 542.
15 Z. F. Chen and T. J. Meyer, *Angew. Chem., Int. Ed.*, 2013, **52**, 700.
16 M. M. Najafpour, T. Ehrenberg, M. Wiechen and P. Kurz, *Angew. Chem. Int. Ed.*, 2010, **49**, 2233.

17 a) K. S. Joya and H. J. M. de Groot, *ACS Catalysis*, 2016, **6**, 1768; b) M. Dincă, Y. Surendranath and D. G. Nocera, *Proc. Natl. Acad. Sci. U.S.A.*, 2010, **107**, 10337.
18 a) C. W. Li and M. W. Kanan, *J. Am. Chem. Soc*., 2012, **134**, 7231; b) Y. Chen and M. W. Kanan, *J. Am. Chem. Soc*., 2012, **134**, 1986.
19 Z. F. Chen, J. J. Concepcion, M. K. Brennaman, P. Kang, M. R. Norris, P. G. Hoertz and T. J. Meyer, *Proc. Natl. Acad. Sci. U. S. A.*, 2012, **109**, 15606.
20 M. W. Kanan and D. G. Nocera, *Science*, 2008, **321**, 1072.
21 K. S. Joya, Y. F. Joya and H. J. M. de Groot, *Adv. Energy Mater*., 2014, **4**, 1301929.
22 K. S. Joya and H. J. M. de Groot, *J. Raman Spec*., 2013, **44**, 1195.
23 K.S. Joya and X. R. Sala, *Phys. Chem. Chem. Phys.*, 2015, **17**, 21094.
24 D. González-Flores, I. Sánchez, I. Zaharieva, K. Klingan, J. Heidkamp, P. Chernev, P. W. Menezes, M. Driess, H. Dau and M. L. Montero, *Angew. Chem. Int. Ed.*, 2015, **54**, 2472.
25 T. M. Lopez, J. R. Vilche and A. J. Arvia, *J. Appl. Electrochim.*, 1988, **18**, 691.
26 T. M. Lopez, J. R. Vilche and A. J. Arvia, *J. Electronal. Chem*., 1984, **162**, 207.
27 K. S. Joya, K. Takanabe and H. J. M. de Groot *Adv. Energy Mater*., 2014, **4**, 1400252.
28 A. M. Ferraria, A. P. Carapeto and A. M. Botelho do Rego, *Vacuum*, 2012, **86**, 1988.
29 J. B. Gerken, E. C. Landis, R. J. Hamers and S. S. Stahl, *ChemSusChem*, 2010, **3**, 1176.
30 J. E. Cloud, L. W. Taylor, Y. Yang, *RSC Adv.*, 2014, **4**, 24551.
31 S. Mao, G. Lub and J. Chen, *Nanoscale*, 2015, **7**, 6924.
32 D. Kim, J. Resasco, Y. Yu, A. M. Asiri and P. Yang, *Nat. Commun.*, 2014, **4**, 5948.
33 S. Y. Lee, D. González-Flores, J. Ohms, T. Trost, H. Dau, I. Zaharieva and P. Kurz, *ChemSusChem*, 2014, **7**, 3442.
34 Y. Li, L. Zhang, X. Xiang, D. Yan and F. Li, *J. Mater. Chem. A*, 2014, **2**, 13250.
35 N. M. AlYami, A. P. LaGrow, K. S. Joya, J. Hwang, K. Katsiev, D. H. Anjum, Y. Losovyj, L. Sinatra, J. Y. Kim and O. M. Bakr, *Phys. Chem. Chem. Phys.*, 2016, **18**, 16169.